THE JOURNAL OF COMPARATIVE NEUROLOGY 405:543–552 (1999)

Three-Dimensional Reconstruction of the Antennal Lobe in *Drosophila melanogaster*

P.P. LAISSUE,[1] C. REITER,[2] P.R. HIESINGER,[2] S. HALTER,[1] K.F. FISCHBACH,[2] AND R.F. STOCKER[1]*

[1]Institute of Zoology and Program in Neuroscience, University of Fribourg, CH-1700 Fribourg, Switzerland

[2]Institut für Biologie III, Albert-Ludwigs-Universität Freiburg, D-79104 Freiburg, Germany

ABSTRACT

We present the first three-dimensional map of the antennal lobe of *Drosophila melanogaster*, based on confocal microscopic analysis of glomeruli stained with the neuropil-specific monoclonal antibody nc82. The analysis of confocal stacks allowed us to identify glomeruli according to the criteria shape, size, position, and intensity of antibody labeling. Forty glomeruli were labeled by nc82, eight of which have not been described before. Three glomeruli previously shown exclusively by backfills were not discernible in nc82 stainings. We distinguish three classes of glomeruli: (1) "landmark" glomeruli that are constant in all four criteria mentioned above, (2) less well-demarcated glomeruli that deviate in a single criterion, and (3) poorly defined glomeruli that vary in more than one criterion. All class 2 and 3 glomeruli can be identified by comparison with landmark neighbors. To further aid identification, our model assigns glomeruli to five arrays, each of which is defined by a prominent landmark glomerulus. Six glomeruli consist of distinct, but contiguous structural units, termed "compartments." Glomerular variability observed occasionally between males and females is in the same range as between individuals of the same sex, suggesting the lack of a significant sexual dimorphism in the glomerular pattern. We compare the new model with a previous map and address its potential for mapping activity and expression patterns. An important goal of this work was to create three-dimensional reference models of the antennal lobe, which are accessible on-line. J. Comp. Neurol. 405:543–552, 1999.

Indexing terms: olfactory system; glomeruli; confocal microscopy; enhancer trap lines; rendering; VRML

The antennal lobe (AL) is the primary olfactory association center in insects. It collects afferents from the principal olfactory appendage, the antenna, and from minor olfactory epithelia, i.e., the labial palps in butterflies (Lee and Altner, 1986; Kent et al., 1986) and the maxillary palps in flies (Singh and Nayak, 1985). In the vast majority of insects, ALs are subdivided into structural units, i.e., the glomeruli (Rospars, 1988; Boeckh and Tolbert, 1993). Glomeruli are the sites of synaptic integration between the terminal branches of olfactory afferents and the dendritic arborizations of their target interneurons. Olfactory interneurons are composed of two major classes: local interneurons, intrinsic to the AL; and projection neurons (PNs), which connect the AL with higher brain centers.

The distinctness of glomeruli varies greatly among different species. In cockroaches (Ernst et al., 1977), honeybees (Arnold et al., 1985), and lepidopterans (Rospars, 1983), glomeruli are very prominent. In flies, they are much less evident (Power, 1946; Strausfeld, 1976), perhaps because the AL lacks an elaborate glial sheath (Stocker et al., 1983, 1990). Also, there are great species-specific differences in their numbers, ranging from 35 glomeruli in *Aedes aegypti* (Bausenwein and Nick, 1998) to 156 in the honeybee (Flanagan and Mercer, 1989; Galizia et al., 1999), and up to 1,000 in locusts or wasps (Rospars, 1988). Species that were studied in detail re-

Grant sponsor: Bundesministerium für Bildung, Wissenschaft, Forschung und Technologie, Grant number: 0310959; Grant sponsor: Swiss National Funds; Grant number: 31–42053.94; Grant number: 31–52639–97; Grant sponsor: Human Frontier Science Program; Grant numbers: RG-93/94 B, 259–873–02.

*Correspondence to: Dr. Reinhard F. Stocker, Institute of Zoology and Program in Neuroscience, University of Fribourg, CH-1700 Fribourg, Switzerland. E-mail: Reinhard.Stocker@unifr.ch

Received 5 May 1998; Revised 14 October 1998; Accepted 20 October 1998

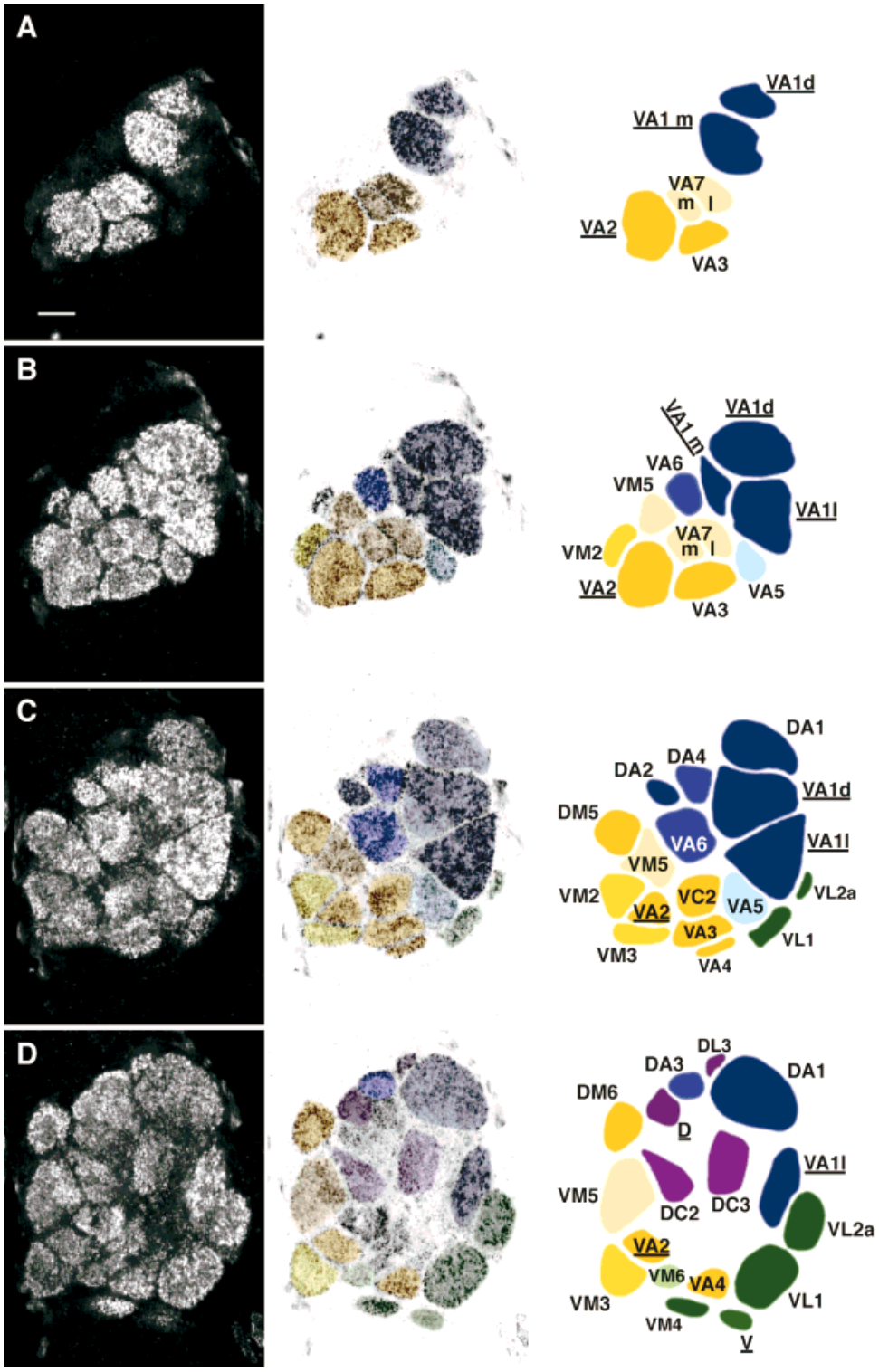

Fig. 1. Representative confocal stack of the antennal lobe (AL) of *D. melanogaster* as shown by mab nc82 staining. Seven frontal planes through a male AL from anterior to posterior (A–G) were selected, from a total of 134 images at 0.34-µm intervals. Lateral is to the right, dorsal on top. Left columns: Unaltered confocal images (primary dataset). Middle columns: Demarcated glomeruli and compartments (in color) superimposed on confocal images with inverted gray-scale. Right columns: Identified glomeruli and compartments (for terminology, see MATERIALS AND METHODS section). Colors indicate the five glomerular arrays VA1 (blue), VA2 (yellow), D (purple), V (green), and DM3 (red), each of which is defined by a corresponding "principal" glomerulus (underlined). Color-coding is identical to that of the Virtual Reality Modeling Language (VRML)-model (Fig. 2). In each of the five colors, dark shading indicates "landmark" glomeruli (class 1), intermediate shading indicates "class 2" glomeruli, and light shading indicates ill-defined glomeruli (class 3). **A:** Frontalmost VA2 array and two compartments of principal glomerulus VA1. **B:** VA1 and VA2 arrays, contributing to the anterior portion of the AL. Note intense staining of all glomeruli. **C:** VA1 and VA2 arrays. Two members of V array appear ventrolaterally. **D:** Posterior part of VA1 and VA2 arrays. Beginning of D and V arrays. **E:** Last members of VA1 and VA2 arrays. First member of DM3 array and peripheral glomeruli of D and V arrays, which compose the "middle" portion of the AL. Note intensely labeled DL3, VM4. and isolated V. **F:** DM3 and V arrays and the posterior ends of DA1 and DL3. Encircled numbers 1 and 2 indicate extra glomeruli (see text). Note bright DM3 and coarse central neuropil. **G:** Posterior portion of DM3 array (principal glomerulus no longer visible). The asterisk indicates the approximate position of VP1–3 (cf. Stocker et al., 1990). Structures on top of (G) do not belong to the AL. Scale bar = 10 µm in A (applies to A–G).

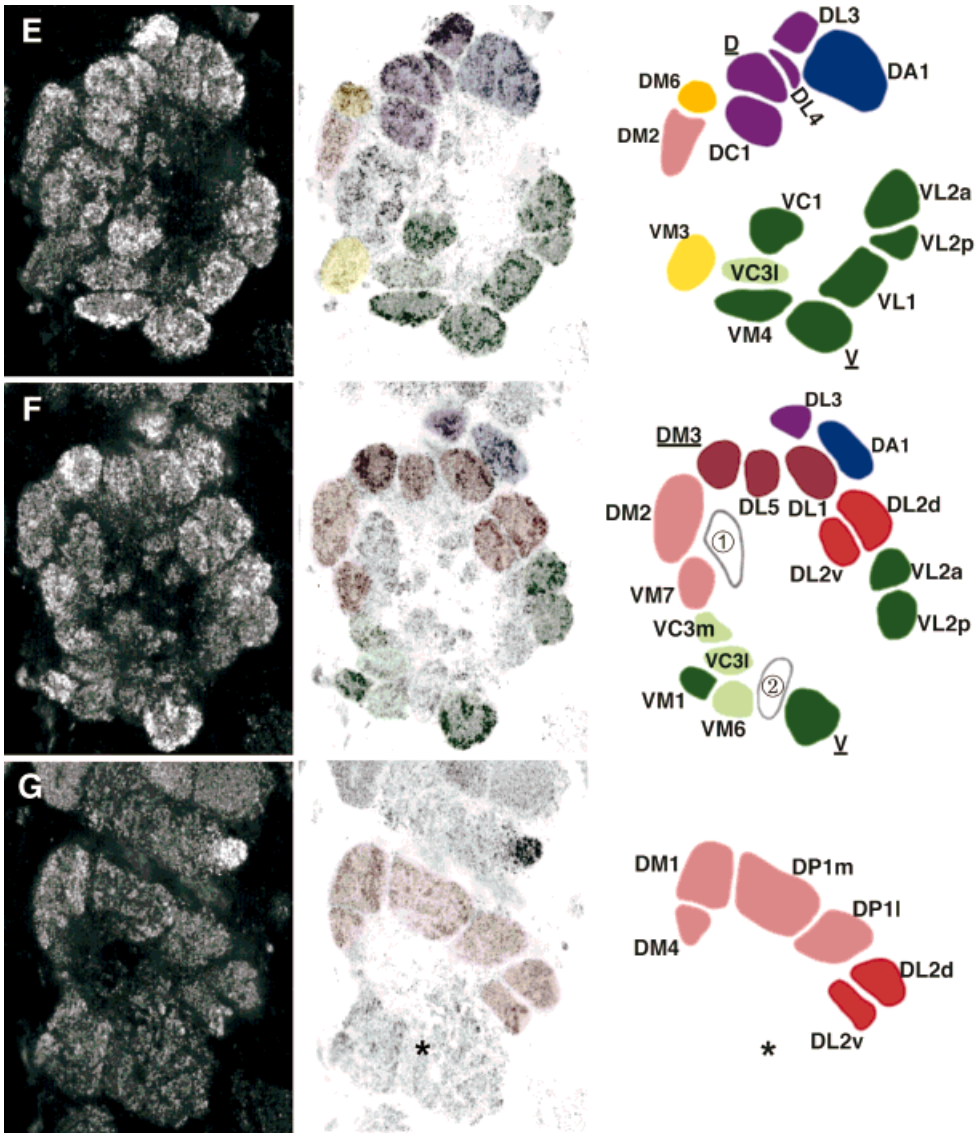

Figure 1 (Continued)

vealed largely invariant numbers and positions of glomeruli, leading to the concept of identifiable glomeruli (Rospars, 1988). In cockroaches, bees, and moths, the glomerular map is clearly sexually dimorphic (Rospars, 1988; Homberg et al., 1989; Rospars and Chambille, 1990; Boeckh and Tolbert, 1993; Hildebrand and Shepherd, 1997), whereas in *Drosophila melanogaster* no such difference was observed (Stocker et al., 1990; Stocker, 1994).

Recent comparisons between insects and vertebrates have revealed surprising parallels in the organization, function, and development of the olfactory system (Hildebrand and Shepherd, 1997). This has renewed the importance of insects as model systems for olfactory research. *Drosophila* has become a particularly attractive model due to the striking progress in molecular genetic techniques. For example, enhancer trap strains (Brand and Dormand, 1995) should facilitate the isolation, mapping, and characterization of genes that are expressed in the olfactory system. Moreover, they are excellent cell-specific neuronal markers that allow investigation of the anatomy, function, and development of the system. As an up-to-date anatomical reference for such studies, we have created a new map of the AL of *D. melanogaster*. A previously published model relied on labeled afferents and PNs and on autofluorescence in tissue sections (Stocker et al., 1983, 1990; Pinto et al., 1988). The map we present here is based on the improved resolution of glomeruli by monoclonal antibody staining, confocal microscopy, and three-dimensional (3D) image processing.

We compare our new model with the previous map; we discuss issues of glomerular variability, sexual dimorphism, and reconstruction parameters; and we address possible applications to enhancer trap expression patterns and functional maps. A 3D model of our reconstruction that can be manipulated on-line is accessible through the "Flybrain" image database (accession number AB00200, at http://www.flybrain.org; cf. Armstrong et al., 1995). Glomerular maps of the AL have been created also in the

honeybee (Flanagan and Mercer, 1989; Galizia et al., 1999) and *Aedes aegypti* (Bausenwein and Nick, 1998).

MATERIALS AND METHODS

Fly stocks

Canton-S flies were raised at room temperature (RT) in noncrowding condition with a 12 hour light/12 hour dark cycle. They were killed between 10 hours and 6 days after eclosion.

Antibody staining of the brain

We tested a selection of monoclonal antibodies (mabs), i.e., aa2, ab49, nb141, and nc82, all kindly provided by Dr. A. Hofbauer, University of Regensburg, which were previously shown to bind to various parts of the brain (Hofbauer, 1991). The mab nc82, which recognizes neuropil structures, showed the most distinct staining of glomeruli.

Flies were fixed in 4% paraformaldehyde containing 0.2% Triton X-100 for 3 hours on ice and washed for 3 hours with phosphate buffered saline containing 0.2% Triton X-100 (PBST). Brains were then dissected and blocked with 3% normal goat serum in PBST (RT, 1 hour). nc82 was diluted 1:10 (volume/volume) in the blocking solution (3% normal goat serum in PBST) and incubated overnight at RT with gentle shaking. After a brief rinse in PBST, an anti-mouse F(ab')2 antibody coupled to the indocarbocyanine fluorophore Cy3 (Jackson Immuno-Research Laboratories, West Grove, PA) was applied 1:100 (volume/volume) in the blocking solution for 4 hours at RT. After rinsing in PBST, brains were mounted in Vectashield (Vector Laboratories, Burlingame, CA). To protect brains from pressure by the coverslip, they were placed into spacer rings of approximately 120 µm in height. The coverslips were sealed with rubber cement ("Fixogum," Marabuwerke GmbH & Co., D-71732 Tamm).

Confocal microscopy

Whole-mounts of the brain were studied with a Leica TCS 4D and a BioRAD MRC 1024 confocal microscope, both equipped with a Kr/Ar laser. Frontal series of individual ALs (cf. Fig. 1) were taken at 3 images/µm with 512 × 512 pixel resolution, resulting in an average of 140 images per AL (Pawley, 1990; website: http://www.cs.ubc.ca/spider/ladic/confocal.html). ALs from 18 female and 16 male brains were analyzed and compared. Eight representative confocal image series of the AL (four females, four males) were processed for 3D analysis. Those are used as reference specimens in this study.

Analysis of confocal stacks and reconstruction

We used two sets of hardware and software: A Silicon Graphics Octane workstation equipped with the image processing programs Amira (Konrad-Zuse-Zentrum für Informationstechnik, Berlin), Imaris (Bitplane AG, Zürich), and CosmoWorlds (Silicon Graphics, Inc., Mountain View, CA), as well as a Power Macintosh 8500/150 with the public domain NIH Image program (written by Wayne Rasband at National Institutes of Health and available from the Internet from http://rsb.info.nih.gov/nih-image).

Each stack of digital images was analyzed with the following techniques (see DISCUSSION section). (1) Volume rendering (Fig. 3): The raytracing algorithm implemented in Imaris was used to reconstruct views of the entire object from defined camera positions. Animations were created by rendering a series of images from progressively shifting viewpoints, e.g., depicting a rotation from a frontal to a posterior viewpoint with 3-µm intervals. (2) Original stacks (Fig. 1) were compared with the volume-rendered views to identify glomerular structures. (3) Surface rendering (Fig. 2): Glomeruli were demarcated by hand in confocal image stacks to define contours, thus producing polygon groups of the surfaces of the glomeruli. The polygon data were exported to the Virtual Reality Modeling Language (VRML V2.0 utf8). The resulting surface models were further processed with CosmoWorlds and optimized for smooth handling on current desktop systems (Russ, 1995; websites: http://biocomp.arc.nasa.gov, http://stanford.edu/3dreconstruction). All figures presented here were produced by using Adobe Photoshop 4.0 (Adobe Systems, Inc.) and a Kodak Digital Science 8650 PS Color Printer (Eastman Kodak Co.).

Terminology of glomeruli

The terminology of glomeruli is based on the one used in the previous map (Stocker et al., 1983, 1990). Briefly, two capital letters denote the general position of a selected glomerulus in the AL (A, anterior; D, dorsal; L, lateral; M, medial; P, posterior; V, ventral). Central glomeruli (C) are defined as having no contact with the AL periphery. A number allows for additional identification, and in those glomeruli that are further subdivided, a small character specifies the glomerular compartment (see below).

RESULTS

New glomerular map

Careful comparison of 34 confocal stacks indicated the presence of 40 glomeruli in the AL of *D. melanogaster* (Figs. 1, 2). Three glomeruli at the posterior edge of the AL, VP1–3 (cf. Fig. 1), which were reported from antennal backfills (Lienhard and Stocker, 1987), could not be recognized in nc82-stained ALs. Thus, the AL now consists of 43 glomeruli, compared with 35 in the earlier model (Stocker et al., 1990). The characteristic shapes, sizes, and locations of many prominent glomeruli identified here by nc82 are well known from sensory projections or from arborization patterns of PNs (Stocker et al., 1983, 1990).

Our results corroborate the presence of all of the previously described glomeruli (except VP1–3), but extend and modify the earlier map in several ways. (1) We discovered eight new glomeruli (Figs. 1, 2; Table 1) . They were situated either in regions consisting of tightly packed glomeruli, like the DM and DL regions, or in the coarse central neuropil, which is difficult to define because it contains small, variable fragments and poorly delimited areas. (2) The superior resolution provided by nc82 allowed us to distinguish between "glomeruli," i.e., structural units that are always well separated from one another, and glomerular "compartments" that are separated by a smaller gap and remain partially attached to each other (Figs. 1, 2; Table 1). Compartments were regularly observed in the six glomeruli DL2, DP1, VA1, VA7, VC3, and VL2. VA1 consists of three compartments, whereas the remainder consist of two compartments each. (3) The intensity of Cy3 fluorescence ("brightness") in nc82

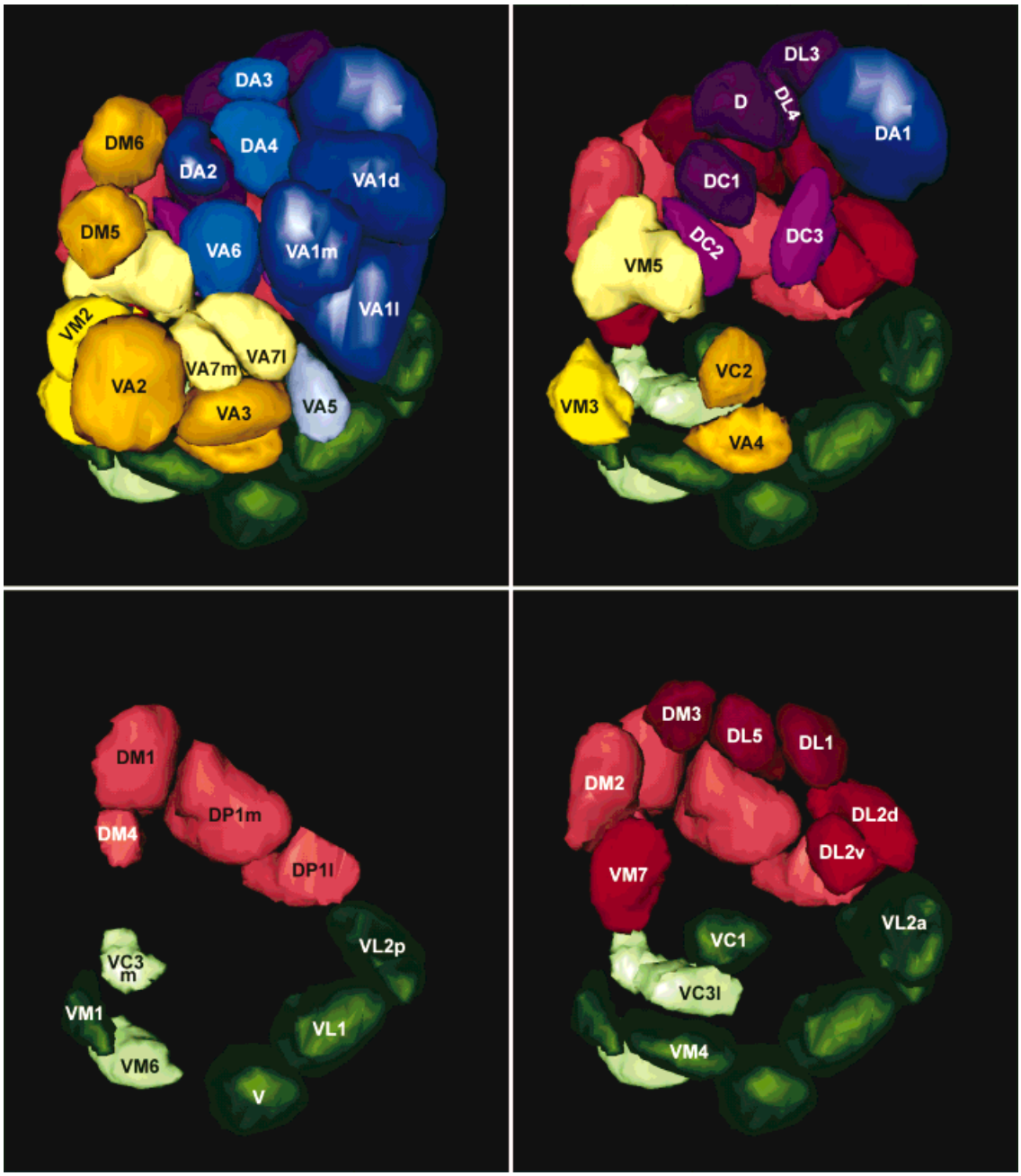

Fig. 2. Virtual Reality Modeling Language (VRML) model of the antennal lobe (AL) as seen from anterior. Lateral is to the right, dorsal on top. Starting clockwise from the complete pattern (top left), the anterior glomeruli are subsequently removed to uncover the underlying central and posterior glomeruli. A total of 40 glomeruli are identified, 6 of which (DL2, DP1, VA1, VA7, VC3, VL2) consist of two to three compartments each ("Flybrain" database Accession Number AB00200 at http://www.flybrain.org).

stainings provided a fourth criterion for glomerular identification, in addition to their size, shape, and position relative to neighboring glomeruli (Fig. 1). (4) Three central glomeruli were found to hold a different position from that described previously. DC1 now appears in a more lateral position, directly ventral of D, and VC1 is seen more medially, just posterior to VC2. The former VC4 is now located medial of DC1 and is renamed DC2, to indicate its new dorsal position. For all other glomeruli, the previous nomenclature (Stocker et al., 1983, 1990) was maintained, even though in some of them the positions differ now slightly compared with the original map.

Close comparison of AL reconstructions from males and females revealed that intrasexual variability in terms of glomerular number and distribution is in the same range as between the two sexes. Hence, neither the glomerular nor the compartment pattern appear to be clearly sexually dimorphic. Also, studying ALs at various adult ages from

TABLE 1. Glomeruli in the Antennal Lobe of *Drosophila melanogaster*[1]

Glomerulus	Compartments	Compared with Stocker et al. (1990)	Array	Class
D			D	1
DA1			VA1	1
DA2			VA1	1
DA3			VA1	2 p
DA4			VA1	2 sz
DC1		More lateral	D	1
DC2		Former VC4	D	2 p
DC3		New	D	2 sh
DL1			DM3	1
DL2	d + v		DM3	2 sh
DL3			D	1
DL4		New	D	1
DL5		New	DM3	1
DM1			DM3	3
DM2			DM3	3
DM3			DM3	1
DM4		New	DM3	3
DM5		New	VA2	1
DM6		New	VA2	1
DP1	m + l		DM3	3
V			V	1
VA1	d + m + l		VA1	1
VA2			VA2	1
VA3			VA2	1
VA4			VA2	1
VA5			VA1	3
VA6			VA1	2 sz
VA7	m + l		VA2	3
VC1		More medial	V	1
VC2			VA2	1
VC3	m + l		V	3
VL1			V	1
VL2	a + p		V	1
VM1			V	1
VM2			VA2	2 sz
VM3			VA2	2 sh
VM4			V	1
VM5			VA2	3
VM6		New	V	3
VM7		New	DM3	2 sz
VP1–3		Not discernible by mab nc82		

[1]Glomeruli and their compartments in the dorsal and ventral half of the antennal lobe (AL). Glomerular nomenclature is based on the terminology of Stocker et al. (1983, 1990) (for details, see Materials and Methods section). New glomeruli, changes in nomenclature and position are indicated. For proper identification, glomeruli are attributed to five arrays, consisting of a principal glomerulus (D, DM3, V, VA1, VA2; underlined) and five to nine glomeruli in its vicinity (cf. Table 2). Classes refer to the distinctness of glomeruli. Class 1 ('landmark') glomeruli are constant in position, shape, size, and staining intensity. Class 2 and 3 glomeruli deviate in one or more than one of these four criteria, respectively (see Results section). Deviations in class 2 glomeruli are indicated in the last columns (p, position; sh, shape; sz, size).

TABLE 2. Glomerular Arrays[1]

AL region	Array	Direction of identification	Sequence of glomeruli in the array
Anterior	VA1	Clockwise, starting dorsally of VA1	DA1-VA1-VA5-VA6 (medial of VA1m)-DA2-DA4 (at dorsomedial tip of VA1d)-DA3
	VA2	Clockwise, dorsal of VA2	VM5-VA7-VC2 (posteroventral of VA7)-VA3-VA4-VA2-VM3-VM2-DM5-DM6 (dorsal of DM5)
	D	Clockwise from D	DL4-DL3-DC3-DC2-DC1-D
	V	Clockwise, dorsal of V	VC1-VL2-VL1-V-VM4-VM6-VM1-VC3
	DM3 anterior	Clockwise, from DM3	DL5-DL1-DL2-VM7-DM2-DM3
Posterior	DM3 posterior	Clockwise, from dorsal	DM1-DP1-DM4

[1]Identification of glomeruli in the five arrays. The indicated sequence of glomeruli in successive frontal sections from anterior to posterior helps to identify glomeruli. For clarity, the DM3 array has been split into an anterior and posterior half. Principal glomeruli are underlined.

10 hours to 6 days after eclosion did not reveal obvious differences in the glomerular pattern.

Visual aid for glomerulus identification

Because the 40 glomeruli vary in terms of relative position, size, shape, and brightness (see above), we distinguished three different classes (Table 1): Twenty-two well-demarcated "landmark" glomeruli are constant in position, size, shape, and brightness. One among them, glomerulus V is distinct by its ventral, isolated location, and serves as a marker for general AL orientation, together with several other prominent glomeruli like D, DM3, VA1, and VA2. Nine "class 2" glomeruli deviate in one of these four criteria (Table 1), whereas the remaining nine "class 3" glomeruli are poorly demarcated and vary in more than one criterion.

To facilitate identification, the 40 glomeruli were assigned to five glomerular "arrays." Arrays are defined by the five most easily identifiable glomeruli, termed "principal" glomeruli (D, DM3, V, VA1, VA2) and up to nine glomeruli in their vicinity (Fig. 1; Table 1). Table 2 indicates the glomerular composition in each array. The VA1 and VA2 arrays comprise the anterior portion of the AL, the V and D arrays occupy its central part, and the DM3 array includes the posterior end of the AL. In our model, the five arrays are labeled by the colors blue, yellow, purple, green, and red, and the three classes of distinctness are shown by different shading (Figs. 1, 2). Arrays and the color code do not suggest specific functions, but are merely intended to help glomerular identification by making small groups. In this way, any glomerulus can be identified by comparing its position relative to the principal glomerulus and the neighboring glomeruli of the same array.

By focusing on single glomeruli, we addressed questions of glomerular identity and variability in more detail (Fig. 3) . Although anterior glomeruli exhibit a uniformly bright fluorescence, posterior ones differ in their intensity, which often facilitates recognition of glomeruli. Hence, in the posterior half of the AL, DL3, DM3, and VM4 can be identified by their exceptional brightness alone. However, the identification of certain class 3 glomeruli was sometimes difficult. Examples are the lack of a clear boundary between DM1 and DM4 or DM2, the faint labeling of DP1 (Fig. 1G) and many central glomeruli, and an ill-defined posterior half of VM5. Although some of these problems may be due to technical reasons (see the DISCUSSION section), there is evidence for natural variability, regarding both glomeruli and compartments. For example, a faintly stained area with a diffuse border was found laterally of DM2 in four of eight reference specimens (Fig. 1F). Also, a small satellite glomerulus was discovered medially of V in two cases (Fig. 1F). Additional compartments in DA4 (Fig. 3A) and VA2 were found in two of the eight reference specimens. VA5 and DL3 (Fig. 3A) had additional compartments in one specimen each. However, only glomeruli and compartments that could be identified unambiguously in all reference specimens are included in the map.

Our map can be used essentially to identify glomeruli in nc82-stained whole-mounts. This identification can be done either by comparing the nc82 label of the unidentified confocal image series to an identified stack (Fig. 1, third row) or by manipulating the 3D surface model on-line in the "Flybrain" image database (cf. Figs. 2, 4). In addition, the map may also be helpful for identifying prominent glomeruli visualized by other histologic techniques, although the resolution will be inferior.

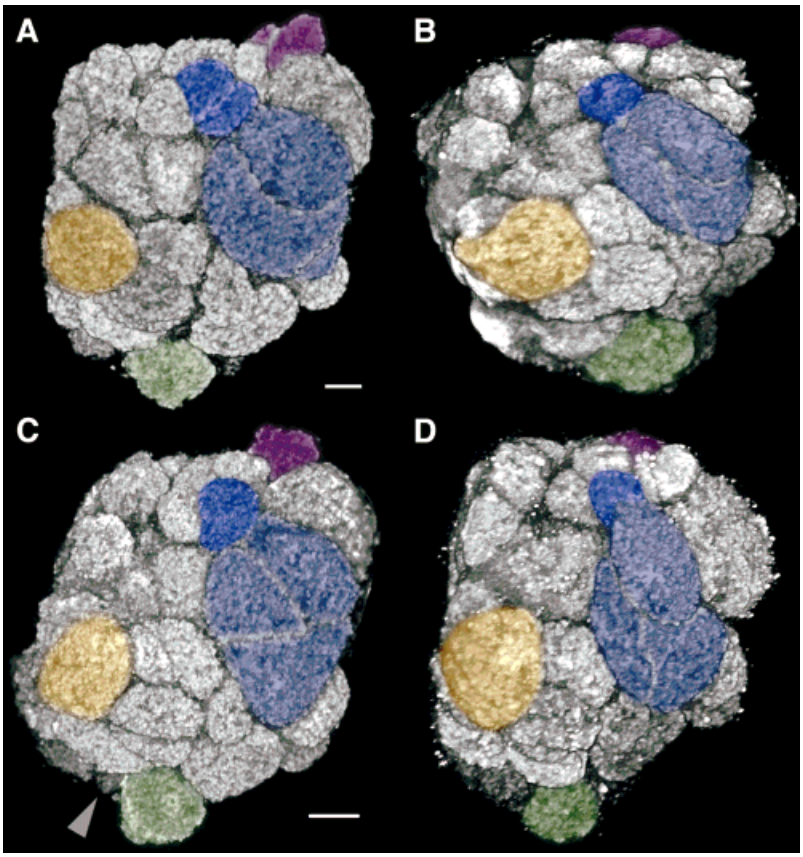

Fig. 3. Variability of glomerular patterns. Volume-rendered views of two female (**A,B**) and two male antennal lobes (ALs) (**C,D**) labeled with mab nc82 (gray scale). The surrounding tissue (cf. Fig. 1) was removed. Demarcated glomeruli are superimposed, their colors corresponding to the model of Figures 1, 2. Principal glomeruli V, VA1, and VA2 are shown in green, dark blue, and yellow, respectively. Glomeruli DL3 (purple) and DA4 (bright blue) exhibit extra compartments in A. The arrowhead in C indicates an additional glomerulus. Another four volume and surface reconstructed ALs from different individuals are available at Flybrain (cf. Fig. 2). Scale bars = 10 μm in A,C (applies to A–D).

DISCUSSION

New glomeruli and compartments

The present study shows that the AL of *D. melanogaster* consists of 43 glomeruli, 40 of which are clearly identifiable by nc82. All the glomeruli of the previous model (Stocker et al., 1990) were confirmed by our observations (except the three glomeruli that are not shown by nc82; see below). Eight glomeruli as well as the existence of compartments in six glomeruli are newly described in this study. The significance of compartments in cellular and functional terms is not clear. In several moth species, afferents and PNs were shown to terminate exclusively in specific subdivisions of the macroglomerular complex (Koontz and Schneider, 1987; Hansson et al., 1991, 1992, 1994; Christensen et al., 1995). It will be interesting to study whether this applies to compartments in *Drosophila* as well. From the three glomeruli that are not stained by nc82, VP2, and VP3 are targets of nonolfactory afferents from the aristal sensillum (Lienhard and Stocker, 1987). The lack of staining in these could be due to less tight clustering of sensory terminals than in ordinary glomeruli.

Variability of the glomerular pattern

Strong evidence for natural variation stems from the rare but unambiguous occurrence of extra glomeruli and compartments, which are for the first time described here in *Drosophila*. Examples are a "satellite" glomerulus medially of V, which is reminiscent of other peripheral glomeruli (Fig. 3C), or additional compartments in peripheral glomeruli, which do not look different than other compartments (Fig. 3A). Variations in the number of glomeruli have been reported in several insects, although the underlying reasons remain unknown (Arnold et al., 1985; Rospars, 1988; Rospars and Chambille, 1990; Rospars and Hildebrand, 1992; Galizia et al., 1999).

There may be methodologic reasons for identification problems with certain class 3 glomeruli, e.g., subtle changes in the strength of antibody binding or difficulties in recognizing glomerular borders when their surface coincides with the plane of section. However, problems in identifying central glomeruli are also certainly due to the coarse, unstructured architecture of the AL core. Central glomeruli are weakly stained throughout and have less well-defined borders than superficial glomeruli, as confirmed also in nc82 stained cryosections (data not shown). Still, DC1–3 and VC1–3 could be distinguished reproducibly. Other structures that were also observed in the center were not mapped because of their random distribution or because they were present in only a few of the ALs examined.

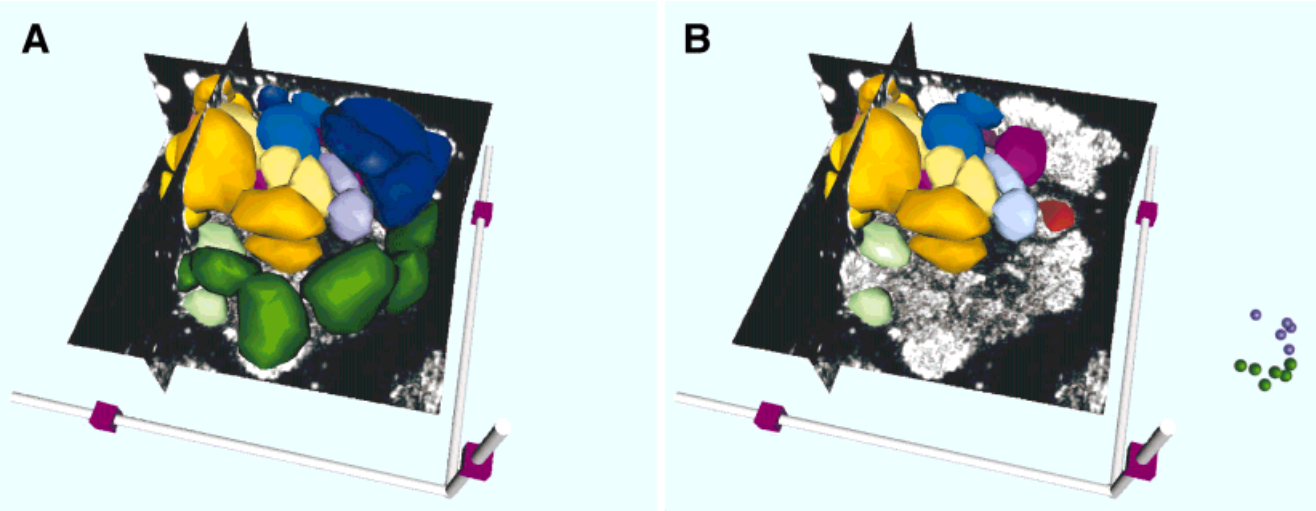

Fig. 4. Interactive Virtual Reality Modeling Language (VRML97) model of the antennal lobe (AL), available at Flybrain (cf. Fig. 2). All glomeruli are shown as reconstructed surfaces. On-line, they can be moved, rotated, and removed by clicking. In addition, images of the primary data set (z axis, anteroposterior) and interpolated views of sagittal and horizontal sections are integrated. They can be displaced within the model by moving the violet boxes on the corresponding axis. **A:** Slightly rotated frontal view. Images of sections are moved to arbitrary positions. **B:** Same view and position of images, but after removal of the landmark glomeruli of two arrays (dark green and dark blue) by clicking. Instead, little balls have appeared at corresponding positions to the right. The glomerulus reappears by clicking on the corresponding ball. All these manipulations of the VRML model can be performed with SGI Cosmo Player and Intervista WorldView on every computer platform.

Comparison of male and female ALs revealed that the intersexual variability in the pattern of glomeruli or compartments is not more pronounced than the intrasexual variability. These observations support earlier data about the lack of a structural sexual dimorphism in the AL of *D. melanogaster* (Stocker et al., 1990). However, because the pattern of trichoid and basiconic sensilla on the antenna is significantly different in the two sexes (Stocker, 1994), connectivity in the AL must be sexually dimorphic. In support of this idea, feminization of specific AL regions in male flies leads to changes in courtship behavior (Ferveur et al., 1995). In contrast to *D. melanogaster*, glomeruli DM1 and DM2 in the Hawaiian species *D. heteroneura* and *D. silvestris* were found to be larger in females than in males (Kondoh and Yamamoto, 1998). This observation may be related to considerably higher numbers of antennal afferents in females (D. Yamamoto, personal communication), which is not the case in *D. melanogaster* (Stocker, 1994). Sexually dimorphic ALs are well known also from cockroaches, bees, or moths, which exhibit a male-specific macroglomerular complex (Rospars, 1988; Homberg et al., 1989; Rospars and Chambille, 1990; Boeckh and Tolbert, 1993; Hildebrand and Shepherd, 1997).

No striking changes in the glomerular pattern from 10 hours to 6 days of adult life were observed. However, we did not measure glomerular volumes. In the worker bee, significant volume changes in AL glomeruli were reported to occur during adulthood, presumably associated with experience (Winnington et al., 1996; Sigg et al., 1997). In *Drosophila*, considerable postmetamorphic plasticity was observed in Kenyon fibers of the mushroom bodies (Technau, 1984). Thus, despite the lack of prominent changes, glomerular plasticity on a cellular level cannot be excluded during adulthood.

Application of the new model

This new glomerular map proved its usefulness as a reference for the expression pattern of Gal4 enhancer trap lines, which are powerful tools for analyzing developmental issues in the AL (cf. Stocker et al., 1997). By crossing such lines with a UAS-reporter strain, the yeast transcription factor GAL4 drives the expression of the secondary reporter (lacZ, tau, or GFP) in a pattern and timing that depend on the genomic context of the inserted P[Gal4] element (O'Kane and Gehring, 1987; Brand and Perrimon, 1993). Among several enhancer trap lines, we studied line GH146 (Heimbeck et al. 1996; Stocker et al., 1997) and line GH231 (G. Heimbeck, personal communication), which express Gal4 in subsets of PNs and olfactory afferents, respectively. An unequivocal identification of Gal4-positive glomeruli was possible in double-labeled ALs in which nc82 provides the identity of all glomeruli, whereas Gal4/UAS-GFP expression is found in a subset. By referring to an early version of the map, we identified glomeruli and compartments in both lines (Halter et al., 1997).

A second important application will be the identification of glomeruli in functional maps. [^{3}H]2-deoxyglucose labeling has previously demonstrated nonhomogeneous activity patterns in the AL of *Drosophila* after odorant stimulation, suggesting that individual glomeruli may be functionally specialized (Rodrigues, 1988). Calcium imaging techniques that were recently established for the honeybee AL and the zebrafish olfactory bulb (Joerges et al., 1997; Friedrich and Korsching, 1997) may soon be applicable to *Drosophila*. In combination with activity maps, the model may also help to assign possible functional identities to glomerular compartments.

As another powerful use, the map may allow the glomerular localization of a wide variety of markers in a back-

ground labeled by nc82 or other neuropil markers (e.g., synaptotagmin, anti-csp). Dye fills of antennal afferents or patterns of transcript and protein expression in specific parts or neurons of the AL can be referred to the map. For the majority of these techniques, fluorescent markers are available, which allow a rapid examination of double-labeled preparations in the confocal microscope.

Glomerular marker for the AL of *D. melanogaster*

The choice of an appropriate glomerular marker was of prime importance for establishing a 3D map of the AL, because the borders of glomeruli in the AL of *D. melanogaster* are not very distinct. Thus, from a large library of mabs generated from the *Drosophila* brain (Hofbauer, 1991), we have chosen the neuropil-specific mab nc82 because of its distinct glomerular staining. Other methods, such as autofluorescence, classic stains, antennal backfills with various tracers, and afferent- or interneuron-specific P[Gal4] enhancer trap lines are less suited, either because the resolution of glomeruli is unsatisfactory or only subsets of glomeruli are stained (cf. Stocker et al., 1990). Although choline acetyltransferase (Buchner et al., 1986) and NO synthase patterns (Müller, 1997) show distinct glomeruli, they also label subsets only.

Applicability of 3D reconstruction techniques for the analysis of confocal image series

We show here that confocal microscopy combined with advanced image treatment allows analysis of the 3D structure of the AL in more detail than previous methods (Stocker et al., 1990). Confocal microscopy offers improved contrast and resolution and a smaller thickness of sections without loss of relevant data for 3D reconstruction. The earlier model was established from 16 sections of 4-μm thickness (Stocker et al., 1990), whereas the data presented here rely on up to 170 sections of 0.34-μm thickness. Furthermore, the primary dataset, a series of confocal images, is digital and has aligned sections. This technique provides an ideal basis for the different types of 3D reconstructions available (Russ, 1995). On the one hand, we created surface-rendered images (Fig. 2). They have the appearance of real, physical objects and, therefore, communicate easily to the viewer. On the other hand, we converted 2D images to 3D values by using a volumetric display (volume rendering; Fig. 3).

Surface-rendered models consist only of the idealized surfaces of structures that were demarcated by hand in the primary dataset (Fig. 1) (Russ, 1995). These models contain all data necessary to assemble a view of the reconstruction from any arbitrary direction and can be examined and manipulated on current desktop computers. Therefore, we created "portable" surface models of selected ALs for interactive analysis of the glomerular organization. We applied the VRML, an ISO-standardized 3D description language that allows viewing and manipulation of the reconstructed object with freely distributed software. VRML was developed for presentation of 3D data on the Internet and, thus, is ideally suited for creating a 3D anatomical atlas available to the research community. Furthermore, the new VRML standard (VRML97, utf8) allows interactive programming such as the embedding of original and interpolated confocal data into the surface model (Fig. 4). This process permits reslicing of the primary dataset of frontal sections of the AL in the horizontal and sagittal plane.

Volume rendering produces views of the entire 3D object (Fig. 3) (Russ, 1995). For this technique, we used "ray tracing." This algorithm basically calculates a brightness based on light being absorbed as it travels through the data set. In contrast to surface rendering, the calculation of such views requires relatively high computational power. In this study, we analyzed primary datasets of more than 40 MB each. We applied raytracing to obtain standardized views of the datasets from a series of different angles as defined by the position of a virtual camera. Direct comparison of unprocessed confocal stacks is often complicated by slightly varying angles of sectioning. These difficulties are avoided by visualizing the individual confocal stack as a volume-rendered 3D object. Progress in computer technology may ultimately allow one to investigate models with real-time volume rendering on desktop computers.

ACKNOWLEDGMENTS

We are very grateful for useful comments on the manuscript by Dr. Jean A. Laissue and James N. Joyce. Dr. Fischbach received support from the Bundesministerium für Bildung, Wissenschaft, Forschung und Technologie. Dr. Stocker received support from the Swiss National Funds and Human Frontier Science Program.

LITERATURE CITED

Armstrong JD, Kaiser K, Müller A, Fischbach KF, Merchant N, Strausfeld NJ. 1995. Flybrain, an on-line atlas and database for the *Drosophila* nervous system. Neuron 15:17–20.

Arnold G, Masson C, Budharugsa S. 1985. Comparative study of the antennal lobes and their afferent pathways in the worker bee and the drone (*Apis mellifera*). Cell Tissue Res 242:593–605.

Bausenwein B, Nick P. 1998. Three-dimensional reconstruction of the antennal lobe in the mosquito *Aedes aegypti*. Proceedings of the 26th Göttingen Neurobiology Conference. Stuttgart & New York: Georg Thieme. p 386.

Boeckh J, Tolbert LJ. 1993. Synaptic organization and development of the antennal lobe in insects. Microsc Res Tech 24:260–280.

Brand AH, Dormand EL. 1995. The GAL4 system as a tool for unravelling the mysteries of the *Drosophila* nervous system. Curr Opin Neurobiol 5:572–578.

Brand AH, Perrimon N. 1993. Targeted gene expression as a means of altering cell fates and generating dominant phenotypes. Development 118:401–415.

Buchner E, Buchner S, Crawford G, Mason WT, Salvaterra PM, Sattelle DB. 1986. Choline acetyltransferase-like immunoreactivity in the brain of *Drosophila melanogaster*. Cell Tissue Res 246:57–62.

Christensen TA, Harrow ID, Cuzzocrea C, Randolph PW, Hildebrand JG. 1995. Distinct projections of two populations of olfactory receptor axons in the antennal lobe of the sphinx moth *Manduca sexta*. Chem Senses 20:313–323.

Ernst KD, Boeckh J, Boeckh V. 1977. A neuroanatomical study on the organization of the central antennal pathways in insects: II. Deutocerebral connections in *Locusta migratoria* and *Periplaneta americana*. Cell Tissue Res 176:285–308.

Ferveur JF, Störtkuhl KF, Stocker RF, Greenspan RJ. 1995. Genetic feminization of brain structures and changed sexual orientation in male *Drosophila*. Science 267:902–905.

Flanagan D, Mercer AR. 1989. An atlas and 3-D reconstruction of the antennal lobes in the worker honey bee, *Apis mellifera* L. (Hymenoptera: Apidae). Int J Insect Morphol Embryol 18:145–159.

Friedrich RW, Korsching SI. 1997. Combinatorial and chemotopic odorant coding in the zebrafish olfactory bulb visualized by optical imaging. Neuron 18:737–752.

Galizia CG, McIlwrath SL, Menzel R. 1999. A digital three-dimensional atlas of the honeybee antennal lobe based on optical sections acquired by confocal microscopy. Cell Tissue Res 295:383–394.

Halter S, Heimbeck G, Laissue PP, Reiter C, Stocker RF. 1997. Plasticity of the glomerular pattern and of the contralateral connectivity in the antennal lobe of *Drosophila*. Proceedings of the 25th Göttingen Neurobiology Conference. Stuttgart & New York: Georg Thieme. p 415.

Hansson BS, Christensen TA, Hildebrand JG. 1991. Functionally distinct subdivisions of the macroglomerular complex in the antennal lobe of the male sphinx moth *Manduca sexta*. J Comp Neurol 312:264–278.

Hansson BS, Ljungberg H, Hallberg E, Löfstedt C. 1992. Functional specialization of olfactory glomeruli in a moth. Science 256:1313–1315.

Hansson BS, Anton S, Christensen TA. 1994. Structure and function of antennal lobe neurons in the male turnip moth, *Agrotis segetum* (Lepidoptera: Noctuidae). J Comp Physiol A 175:547–562.

Heimbeck G, Halter S, Python F, Stocker RF. 1996. Enhancer trap lines GH146 and GH298 reveal specific elements of the olfactory system of *Drosophila melanogaster*. Proceedings of the 24th Göttingen Neurobiology Conference. Stuttgart & New York: Georg Thieme. p 266.

Hildebrand JG, Shepherd GM. 1997. Mechanisms of olfactory discrimination: converging evidence for common principles across phyla. Annu Rev Neurosci 20:595–631.

Hofbauer A. 1991. Eine Bibliothek monoklonaler Antikörper gegen das Gehirn von *Drosophila melanogaster*. Habilitation thesis, University of Würzburg, Würzburg, Germany.

Homberg U, Christensen TA, Hildebrand JG. 1989. Structure and function of the deutocerebrum in insects. Annu Rev Entomol 34:477–501.

Joerges J, Küttner A, Galizia CG, Menzel R. 1997. Representations of odours and odour mixtures visualized in the honeybee brain. Nature 387:285–288.

Kent KS, Harrow ID, Quartaro P, Hildebrand JG. 1986. An accessory olfactory pathway in *Lepidoptera*: the labial pit organ and its central projections in *Manduca sexta* and certain other sphinx moths and silk moths. Cell Tissue Res 245:237–245.

Kondoh Y, Yamamoto D. 1998. Sexual dimorphisms in the antennal lobe of two *Drosophila* species. Proceedings of the 26th Göttingen Neurobiology Conference. Stuttgart & New York: Georg Thieme. p 388.

Koontz MA, Schneider D. 1987. Sexual dimorphism in neuronal projections from the antennae of silk moths (*Bombyx mori, Antheraea polyphemus*) and the gypsy moth (*Lymantria dispar*). Cell Tissue Res 249:39–50.

Lee JK, Altner H. 1986. Primary sensory projections of the labial palp-pit organ of *Pieris rapae* L. (Lepidoptera: Pieridae). Int J Insect Morphol Embryol 15:439–448.

Lienhard MC, Stocker RF. 1987. Sensory projection patterns of supernumerary legs and aristae in *D. melanogaster*. J Exp Zool 244:187–201.

Müller U. 1997. The nitric oxide system in insects. Prog Neurobiol 51:363–381.

O'Kane CJ, Gehring WJ. 1987. Detection in situ of genomic regulatory elements in *Drosophila*. Proc Natl Acad Sci USA 84:9123–9127.

Pawley JB, editor. 1990. Handbook of biological confocal microscopy. New York: Plenum Press.

Pinto L, Stocker RF, Rodrigues V. 1988. Anatomical and neurochemical classification of the antennal glomeruli in *Drosophila melanogaster* Meigen (Diptera: Drosophilidae). Int J Insect Morphol Embryol 17:335–344.

Power ME. 1946. The antennal centers and their connections within the brain of *Drosophila melanogaster*. J Comp Neurol 85:485–517.

Rodrigues V. 1988. Spatial coding of olfactory information in the antennal lobe of *Drosophila melanogaster*. Brain Res 453:299–307.

Rospars JP. 1983. Invariance and sex-specific variations of the glomerular organization in the antennal lobes of a moth, *Mamestra brassicae*, and a butterfly, *Pieris brassicae*. J Comp Neurol 220:80–96.

Rospars JP. 1988. Structure and development of the insect antennodeutocerebral system. Int J Insect Morphol Embryol 17:243–294.

Rospars JP, Chambille I. 1990. Identified glomeruli in the antennal lobes of insects: invariance, sexual variation and postembryonic development. In: Singh RN, Strausfeld NJ, editors. Neurobiology of sensory systems. New York & London: Plenum Press. p 355–375.

Rospars JP, Hildebrand JG. 1992. Anatomical identification of glomeruli in the antennal lobes of the male sphinx moth *Manduca sexta*. Cell Tissue Res 270:205–227.

Russ JC. 1995. The image processing handbook. Boca Raton, FL: CRC Press.

Sigg D, Thompson CM, Mercer AR. 1997. Activity-dependent changes to the brain and behavior of the honey bee, *Apis mellifera* (L.). J Neurosci 17:7148–7156.

Singh RN, Nayak S. 1985. Fine structure and primary sensory projections of sensilla on the maxillary palp of *Drosophila melanogaster* Meigen (Diptera: Drosophilidae). Int J Insect Morphol Embryol 14:291–306.

Stocker RF. 1994. The organization of the chemosensory system in *Drosophila melanogaster*: a review. Cell Tissue Res 275:3–26.

Stocker RF, Singh RN, Schorderet M, Siddiqi O. 1983. Projection patterns of different types of antennal sensilla in the antennal glomeruli of *Drosophila melanogaster*. Cell Tissue Res 232:237–248.

Stocker RF, Lienhard MC, Borst A, Fischbach KF. 1990. Neuronal architecture of the antennal lobe in *D. melanogaster*. Cell Tissue Res 262:9–34.

Stocker RF, Heimbeck G, Gendre N, DeBelle JS. 1997. Neuroblast ablation in *Drosophila* P[GAL4] lines reveals origins of olfactory interneurons. J Neurobiol 32:443–456.

Strausfeld NJ. 1976. Atlas of an insect brain. Berlin & New York: Springer Verlag.

Technau GM. 1984. Fiber number in the mushroom bodies of adult *Drosophila melanogaster* depends on age, sex and experience. J Neurogenet 1:113–126.

Winnington A, Napper RM, Mercer AR. 1996. Structural plasticity of the antennal lobes of the brain of the adult worker honey bee. J Comp Neurol 365:479–490.